Angewandte Chemie International Edition

Angewandte International Edition Chemie

GDCh German Chemical Society

How to cite: *Angew. Chem. Int. Ed.* **2026**, 65, e8854855
doi.org/10.1002/anie.8854855

RESEARCH ARTICLE OPEN ACCESS

NiH-Catalyzed Enantioconvergent α-Alkenylation of Carbonyl Compounds via Markovnikov Alkyne Hydronickellation

Hyeontaek Nam[1] | Seji Jang[1] | Dongwook Kim[2] | Sangwon Seo[1]

[1]Department of Physics and Chemistry, DGIST, Daegu, Republic of Korea | [2]Center For Catalytic Hydrocarbon Functionalizations, Institute For Basic Science (IBS), Daejeon, Republic of Korea

Correspondence: Sangwon Seo (sangwon.seo@dgist.ac.kr)

Received: 9 December 2025 | **Revised:** 23 February 2026 | **Accepted:** 3 March 2026

Keywords: alkenylation | alkynes | asymmetric catalysis | nickel | reaction mechanisms

ABSTRACT

β-Methylene carbonyl motifs constitute privileged structural frameworks that play vital roles as a pharmacophore and serve as key intermediates in the assembly of architecturally complex molecules. Despite their synthetic importance, asymmetric approaches for their preparation remain scarce and are largely confined to substrate-controlled or stoichiometric chiral auxiliary methods. Herein, we report a nickel hydride-catalyzed enantioconvergent α-alkenylation of carbonyl compounds with alkynes, providing a direct and general route to α-chiral β-methylene carbonyl derivatives. The transformation proceeds via Markovnikov-selective alkyne hydronickellation followed by nickel-radical recombination to forge the α-stereogenic center, delivering the desired products with high levels of regio- and enantioselectivity. The protocol accommodates a wide range of alkynes and α-halocarbonyl partners, displays excellent functional group tolerance, and can be applied to the modification of biologically relevant molecules. Mechanistic investigations indicate that a partially protic Ni(II)H species governs the observed regioselectivity, while enantio-discrimination occurs during the radical capture step. This work establishes NiH catalysis as a versatile platform for expanding the synthetic repertoire for enantioenriched β-methylene carbonyl architectures.

1 | Introduction

β-Methylene carbonyl motifs and their reduced derivatives constitute privileged structural frameworks that find broad utility across diverse domains of chemical research and synthesis. In particular, those bearing chirality at the α-position are prevalent in natural products and biologically relevant compounds (Scheme 1a) [1–5] and have also been extensively employed as strategic intermediates in the construction of architecturally complex molecules [6–15]. Moreover, the β-methylene unit presents a unique opportunity for multifaceted β-branching transformations by means of alkene functionalization [16–22], thus enhancing molecular complexity in a manner complementary to biosynthetic β-branching pathways that typically rely on the modification of a β-ketone functionality [23]. Given this versatility and synthetic potential, the development of robust and general synthetic methods for accessing such valuable building blocks remains a demanding area of research.

Hyeontaek Nam and Seji Jang contributed equally to this work.

Dedicated to Professor Chulbom Lee on the occasion of his 60th birthday.

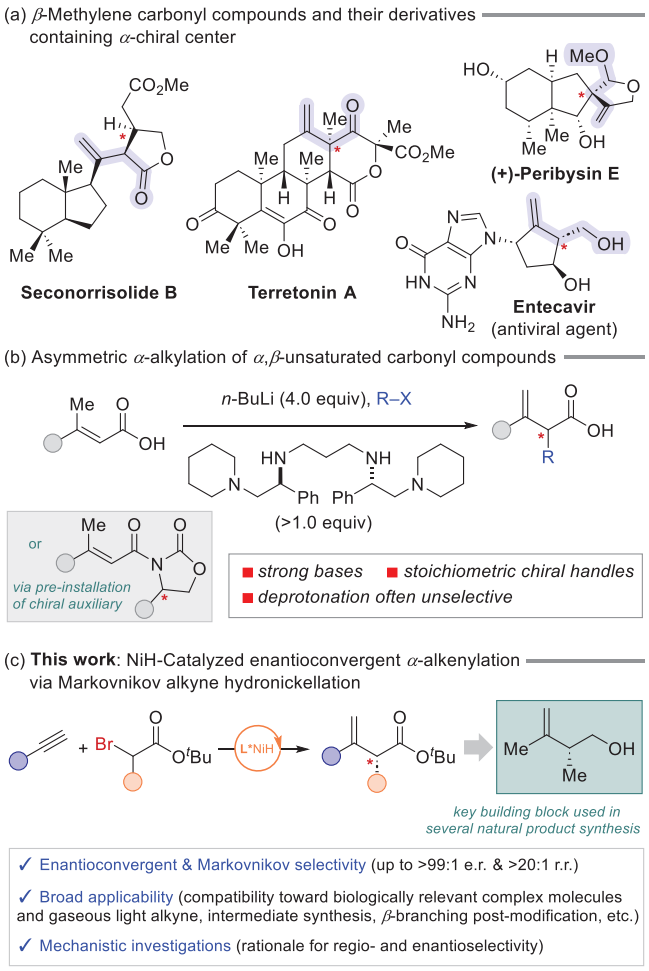

SCHEME 1 | Synthesis of α-enantioenriched β-methylene carbonyl compounds.

Deconjugative α-functionalization of α,β-unsaturated carbonyl compounds may represent the most common strategy for the construction of β-methylene carbonyls [24–29]. Although benefiting from simplicity, this approach is often plagued by narrow structural diversity and the requirement for strong bases. More critically, asymmetric induction within this synthetic platform remains somewhat limited, typically necessitating either the pre-installation of chiral auxiliaries into the reactants [30–36] or in-situ formation of stoichiometric amounts of chiral lithium amides as stereodirecting agents (Scheme 1b) [37–39]. An appealing strategy would be to directly connect the methylene and carbonyl units at the α,β-junction while catalytically promoting asymmetric induction, ideally through functionalization of readily available chemical feedstocks. The catalytic Conia-ene-type reaction, an intramolecular C–C bond-forming process between alkyne (or alkene) and enolizable carbonyl functionality, has enjoyed success in this context [40–45], finding broad applications in natural product synthesis [46–52] and asymmetric catalysis [53–58]. However, the extension of such enantioselective processes to intermolecular variants has lagged behind thus far [59, 60].

In recent years, catalysis based on transition metal hydrides (TMH) has emerged as a new frontier for alkene and alkyne hydrofunctionalization, offering unique reactivity and selectivity that were previously inaccessible by traditional methods [61–70]. We hypothesized that β-methylene carbonyls bearing α-chiral centers could be accessed through systematic optimization of such a catalytic system for Markovnikov-selective alkyne hydrometallation and successive enantioconvergent α-alkenylation of carbonyl compounds (Scheme 1c). In related studies, the Lalic and Fu groups have recently developed elegant copper and cobalt hydride systems that mediate anti-Markovnikov [71] and regiodivergent [72] hydroalkylation reactions, respectively. The latter strategy, in particular, provides a convenient entry to β-methylene amides [72]; however, much of the work was primarily focused on achiral reactions despite the utilization of chiral ligands, thus underscoring the persistent challenges associated with asymmetric catalysis. Furthermore, expanding such systems to accommodate more readily transformable carbonyl motifs, such as esters, is also highly desirable to enable broader diversification and application.

To this end, nickel hydride (NiH) catalysis offers a promising mechanistic platform for the designed asymmetric transformation, given its well-established capability for enantioselective C–C bond formation via hydroalkylation [73–80]. Nonetheless, while NiH-catalyzed enantioconvergent α-alkylation of α-carbon electrophiles have been extensively developed via anti-Markovnikov [81, 82] and remote alkene hydronickellation [82, 83], the alkenylation variant for the asymmetric construction of β-methylene frameworks remains underexplored, with a only single reported example of cyclic substrate that exhibits moderate regioselectivity [81]. The lack of general methods in this context likely stems from the intrinsic challenge that steric features required for effective enantioselectivity control can simultaneously compromise the attainment of Markovnikov selectivity. More recently, alternative strategies employing alkenyl electrophiles have emerged as attractive solutions to potentially circumvent these limitations by pre-defining the reacting site [84, 85]; however, these approaches predominantly rely on 1-alkenyl electrophiles to furnish β,γ-unsaturated linear products. In light of the comparatively limited accessibility of 2-alkenyl electrophiles, the development of a Markovnikov-selective NiH catalytic system for enantioconvergent α-alkenylation using readily available alkynes would provide a complementary and highly valuable approach to α-enantioenriched β-methylene carbonyl compounds.

Herein, we demonstrate that chiral NiH catalysis indeed enables the designed process with high regio- and enantioselectivity, exhibiting broad substrate scope across a wide range of alkynes and α-haloesters (Scheme 1c). The synthetic utility of this method is further evidenced by its excellent functional group tolerance, practicality, and applicability to the modification of biologically relevant molecules and synthesis of a key building block for natural products, as well as by a variety of post-modification, including NiH-catalyzed sequential hydroalkylation for β-branching transformation. Mechanistic investigations suggest that the partial protic character of Ni(II)H may account for the observed regioselectivity, whereas the enantioselectivity is established during the Ni-radical recombination step. Density functional theory (DFT) calculations elucidate the key elements governing enantioselectivity, a mechanistic aspect that has been previously underexplored in NiH-catalyzed enantioconvergent C–C bond formation.

(a) Reaction optimization for achiral reactions[a]

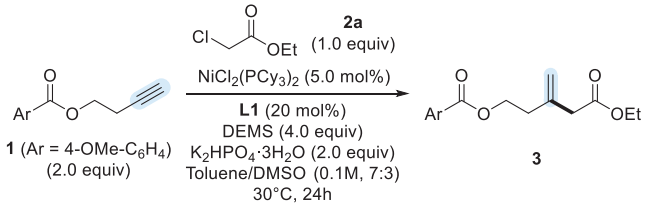

entry	variations from the above conditions	yield (%)
1	none	84
2	$NiCl_2$·glyme instead of $NiCl_2(PCy_3)_2$	50
3	$NiBr_2$·glyme instead of $NiCl_2(PCy_3)_2$	55
4	Toluene/NMP (7:3)	74
5	Toluene/DMA (7:3)	71
6	Toluene/THF (7:3)	65
7	Benzene/DMSO (7:3)	84
8	**L2** instead of **L1**	84
9	**L3** instead of **L1**	n.d.
10	**L4** instead of **L1**	n.d.
11	**L5** instead of **L1**	trace
12	KF instead of $K_2HPO_4·3H_2O$	66
13	15 mol% of **L1** instead of 20 mol%	80
14	Ethyl bromoacetate (**2b**) instead of **2a**	50

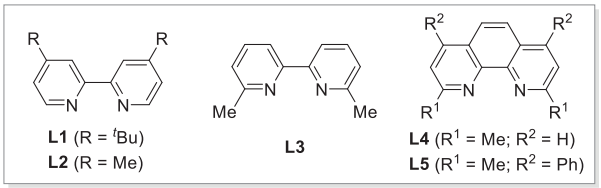

(b) Initial screenings for enantioconvergent reactions[a]

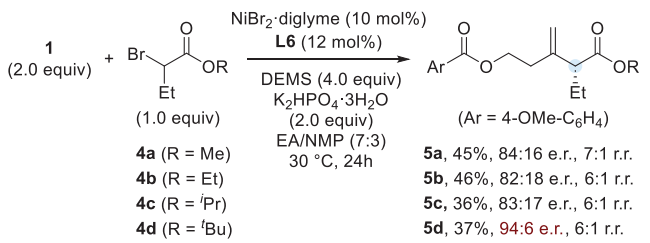

(c) Ligand screenings under modified conditions[a]

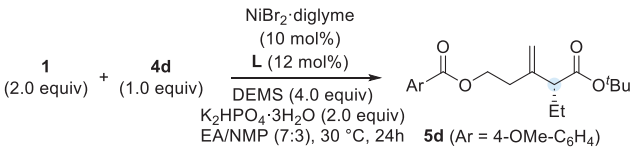

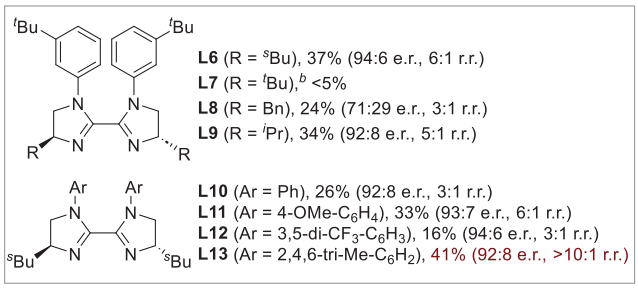

(d) Further optimization[a,c]

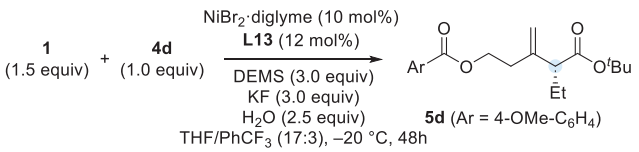

entry	variations from the above conditions	yield (%)	e.r.	r.r.
1	none	91	95:5	>10:1
2[d]	**L6**, EA/NMP (19:1), 30 °C, 24h	71	94:6	7:1
3[d]	**L6**, EA/NMP (19:1), –20 °C, 24h	76	94:6	7:1
4[d]	EA/NMP (19:1) instead of THF/$PhCF_3$	75	95:5	7:1
5[d]	THF instead of THF/$PhCF_3$	86	95:5	8:1
6	30 °C instead of –20 °C	48	95:5	>10:1
7[e]	24h instead of 48h	44	95:5	>10:1

[a]Reaction conditions: Alkyl 2-haloalkanoate (as indicated), alkyne **1** (as indicated), Ni (as indicated), ligand (as indicated), DEMS (as indicated), base (as indicated), H_2O (as indicated) in solvent (1.0 mL) at indicated temperatures under argon atmosphere; Yields determined by ^1H NMR using 1,3,5-trimethoxybenzene as an internal standard; Reported yields are those of the major regioisomers; enantiomeric ratio (e.r.) determined by chiral HPLC analysis. [b]e.r. and r.r. not determined. [c]2.0 mL of solvent instead of 1.0 mL. [d]4 equiv of H_2O instead of 2.5 equiv of H_2O. [e]~50% of **4d** remain unreacted; Cy = cyclohexyl; DEMS = diethoxy(methyl)silane; DMSO = dimethyl sulfoxide; NMP = *N*-methyl-2-pyrrolidone; DMA = *N*,*N*-dimethylacetamide; THF = tetrahydrofuran; n.d. = not detected.

SCHEME 2 | Optimizations of reaction parameters for achiral and enantioconvergent α-alkenylation via alkyne hydronickellation.

2 | Results and Discussion

2.1 | Reaction Optimizations

To achieve a generality for the desired Markovnikov-selectivity first, we commenced our investigation with an achiral system using alkyne **1** and ethyl chloroacetate **2a** as model substrates (Scheme 2a). After extensive screenings of a range of reaction parameters, guided by our previous experience in NiH catalysis [86–89] (see Tables S1–S6 for further details), optimal conditions were obtained with $NiCl_2(PCy_3)_2$ (5 mol%), 4,4'-di-*tert*-butyl-2,2'-bipyridine **L1** (20 mol%), diethoxy(methyl)silane (DEMS; 4.0 equiv), $K_2HPO_4·3H_2O$ (2.0 equiv) as a base, and toluene/DMSO mixture (7:3) as solvent, which led to β-methylene ester **3** in 84% yield and excellent regioselectivity (r.r. >20:1) after 24 h reaction at 30°C (Scheme 2a, entry 1). Alternative sources of nickel precatalysts (Scheme 2a, entries 2 and 3) gave diminished yields, but high Markovnikov-selectivity was maintained in all these cases. Other solvents were generally less effective (Scheme 2a, entries 4–6), except benzene/DMSO combination that gave **3** equally in a high yield (Scheme 2a, entry 7). 4,4'-Dimethyl-2,2'-bipyridine ligand **L2** was found as effective as **L1** (Scheme 2a, entry 8), but the presence of 6,6'-disubstituents on bipyridine (**L3**) and phenanthroline ligands (**L4** and **L5**) resulted in poor reactions (Scheme 2a, entries 9–11). Other bases were less competent (Scheme 2a, entries 12), but the amount of ligand could be reduced to 15 mol% with only negligible loss of efficiency (Scheme 2a, entry 13). Ethyl bromoacetate **2b** could be employed as a replacement of **2a**, albeit giving product **3** in a lower yield (Scheme 2a, entry 14).

With the Ni system proven superior for the desired Markovnikov-selective hydroalkylation, we next wished to explore the feasibility of enantioconvergence of the carbonyl substrates having

an additional α-substituent. Unfortunately, a simple replacement of ligand **L1** with any sort of chiral ligands was unsuccessful under the above optimized conditions (see Tables S7–S16 for full details of optimization investigations). The choice of solvents was found to be more essential in this case, with the combination of ethyl acetate and NMP (7:3) initially allowing for the formation of α-substituted-β-methylene esters **5a–5d** by using biimidazoline (BIIM) ligands (Scheme 2b). Notably, the *O*-substituents on the ester motif displayed substantial effects on the enantioselectivity, improving the enantiomeric ratio (e.r.) as they become bulkier (*vide infra* for mechanistic investigation). For instance, using BIIM ligand **L6** that contains 4,4'-di-*sec*-butyl and *N,N'*-di-(*3-tert*-butyl)phenyl substituents, methyl (**4a**; R = Me), ethyl (**4b**; R = Et), and isopropyl esters (**4c**; R = ^{i}Pr) were converted to the corresponding β-methylene products (**5a–5c**) with moderate enantioselectivities, whereas *tert*-butyl variant **4d** led to **5d** with an improved selectivity (e.r. = 94:6). However, the regioselectivity was diminished under these asymmetric conditions, presumably because the steric constraints of the ligands now interfere with the regiocontrol.

Ligand screening was next performed to improve both the efficiency and selectivity of the reaction between alkyne **1** and 2-bromoalkanoate **4d**, through variation of the 4,4'- and *N,N'*-substituents on the ligands (Scheme 2c). While BIIM ligand bearing bulkier 4,4'-substituents (**L7**; R = *tert*-butyl) significantly deteriorated the reaction, the sterically less demanding analog (**L8**; R = benzyl) afforded the desired product **5d**, albeit in poorer yield and lower selectivity. In contrast, 4,4'-di-isopropyl ligand **L9** delivered comparable results to those obtained with **L6**. Electronic modification at the *N,N'*-aryl groups was also found to be influential (**L10–L12**), with electron-withdrawing substituents leading to poorer reactivity (**L12**). Pleasingly, regioselectivity could be improved by employing ligand **L13** appended with *N,N'*-mesityl groups, although with a slight decrease in enantioselectivity (e.r. = 92:8).

Further optimization studies were carried out using ligands **L6** and **L13**, through which we established effective asymmetric conditions for the designed transformations (Scheme 2d). The optimal protocol employed $NiBr_2$·diglyme (10 mol%), **L13** (12 mol%), DEMS (3.0 equiv), KF (3.0 equiv) as a base, H_2O (2.5 equiv) as additive, and THF/$PhCF_3$ mixture (17:3) as solvent at –20°C. Under these conditions, β-methylene ester **5d** was obtained in 91% yield with excellent regio- (>10:1 r.r.) and high enantioselectivity (95:5 e.r.) after 48 h reaction (Scheme 2d, entry 1). Ligand **L6** also proved effective; 24 h reactions gave consistent results regardless of temperature, albeit in slightly diminished yield and lower regioselectivity when conducted in EA/NMP solvent (Scheme 2d, entries 2 and 3). On the other hand, THF/$PhCF_3$ was identified as a more compatible solvent system for **L13** (Scheme 2d, entries 4 and 5), with which the reaction exhibited greater temperature sensitivity (Scheme 2d, entry 6). The reaction employing **L13** proceeded more slowly at –20°C with minimal decomposition (Scheme 2d, entry 7), which likely accounts for its excellent overall efficiency.

As shown in scheme 2, the present asymmetric system furnishes (*R*)-configured products as the major isomers, later confirmed by x-ray crystallographic analysis and by comparison of the specific rotation of a derivatized product (**66**) with reported data (*vide infra*). It is also noteworthy that the addition of H_2O was not essential when alternative bases were used (see Tables S12–S13), suggesting that H_2O is less likely to participate directly in the catalytic cycle. Although the role of H_2O as a thermodynamic promoter [86] cannot be completely ruled out, it may simply enhance the reaction efficiency by facilitating the solubilization of KF in the reaction medium.

2.2 | Substrate Scope

With the optimized conditions in hand, we first probed the scope of alkynes amenable to the reactions with achiral α-halocarbonyl compounds (Scheme 3, top). Under the optimized conditions employing achiral ligand **L1**, the reaction exhibited excellent compatibility across a wide range of alkynes, showing high functional group tolerance and structural diversity (**3**, **6–22**). As with the standard substrate (**3**), alkynes bearing a benzoate group led to β-methylene esters (**6** and **7**) in good yields. Not only were tosyloxy (**8**), silyloxy (**9**), and acetal (**10**) groups well tolerated, but even subtle functionalities such as free hydroxyl (**11** and **12**) and aldehyde (**13**) could also be successfully incorporated. The generality of the reaction was further demonstrated by compatibility with epoxide (**14**), phthalimide (**15**), and amine (**16**) substrates. Aliphatic alkynes proved to be highly effective regardless of the backbone structure (**17–21**), whereas phenylacetylene afforded β-methylene ester **22** only in moderate yield. The reaction was also applicable to 2-halocarbonyl partners bearing amides (**23** and **24**), cyclic ester (**25**), cyclic amide (**26**), and ketones (**27–32**), generally providing the corresponding β-methylene carbonyl derivatives in moderate to excellent yields. An exception was observed for the secondary amide derivative (**24**), which was hampered by the formation of a semi-reduction side product to result in a comparatively lower yield. This side reaction likely arises from protodenickellation of the alkenyl-Ni intermediate, a process presumably facilitated by the presence of an amide N–H motif.

Our scope investigation was next expanded to the asymmetric system (Scheme 3, bottom). Remarkably, the superb functional group tolerance was retained, delivering high regio- and enantioselectivity across a broad range of alkynes and *tert*-butyl α-bromoesters (**5d** and **33–58**). Outstanding enantioselectivity was achieved for the α-isopropyl-substituted ester, leading to α-enantioenriched products (**33–47**) in excellent enantioselectivity and moderate to good yields. Functional groups that had proven compatible in the achiral system were equally well tolerated in the asymmetric variant (**33–40**), along with newly examined functionalities such as nitrile (**41**), ester (**42**), *N*-(carbonyloxy)succinimide (**43**), and chloro (**44**) groups. Structural diversity with respect to α-bromoesters was also broad: alkyl (**5d** and **48–52**), benzyl (**53** and **54**), and phenethyl (**55**) substituents at the α-position were readily accommodated, yielding the corresponding β-methylene esters with high enantioconvergence in reactions with alkyne **1**. Compatibility of indole (**56**), sulfide (**57**), and ether (**58**) functionalities further underscores the versatility of the present asymmetric process, although somewhat diminished enantioselectivity was observed in the cases of **56** and **58**. Notably, excellent regioselectivity was maintained for most substrates, with only a few exceptions (**36**, **40**, **47**, **49**, and **52**) displaying slightly reduced r.r. without discernible trends.

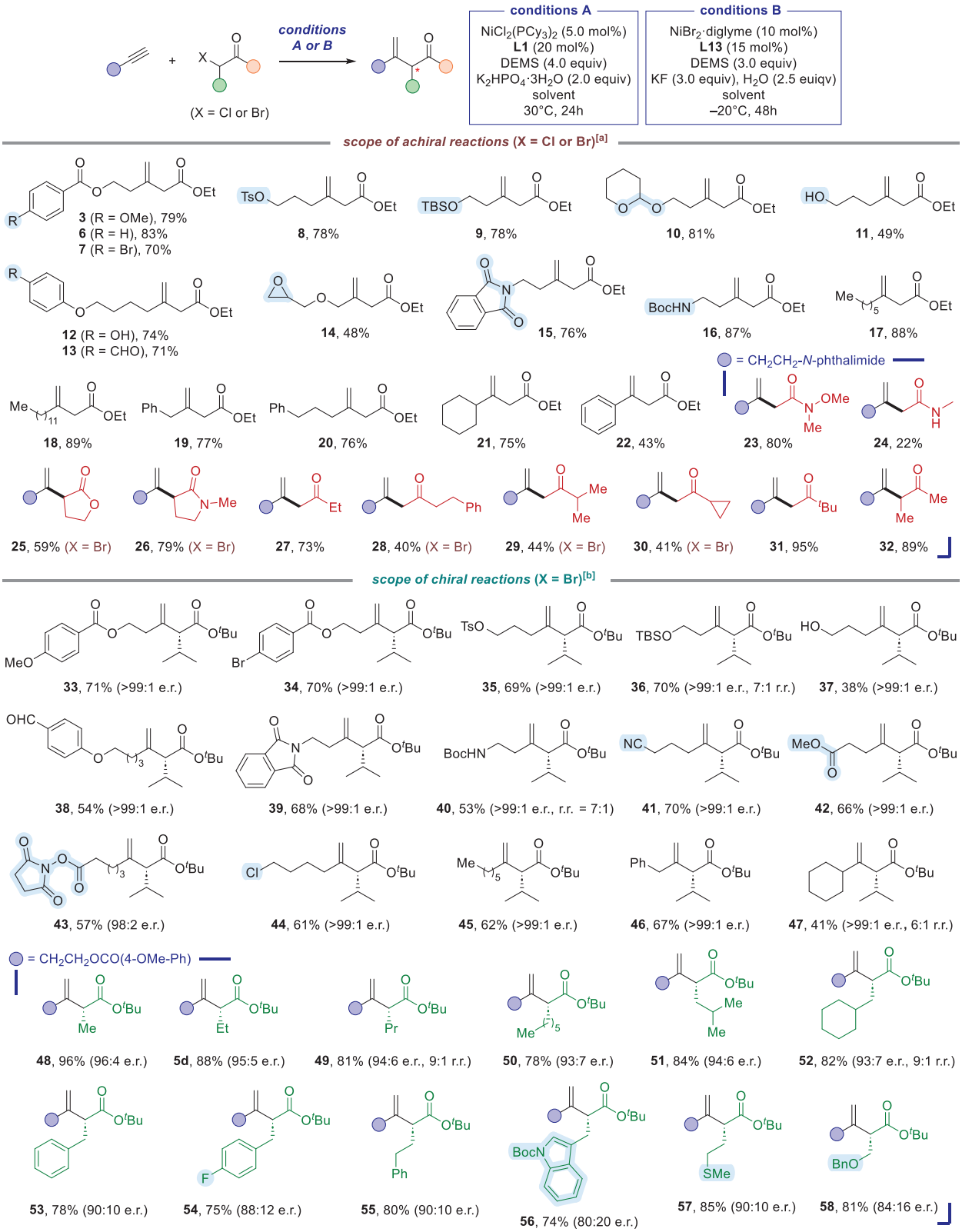

SCHEME 3 | Reaction scope of the α-alkenylation of halocarbonyls via alkyne hydronickellation. [a] **Conditions A**: 2-halocarbonyl compound (0.2 mmol), alkyne (0.4 mmol), $NiCl_2(PCy_3)_2$ (5.0 mol%), **L1** (20 mol%), DEMS (4.0 equiv), and $K_2HPO_4{\cdot}3H_2O$ (2.0 equiv) in toluene/DMSO (7:3, 2.0 mL) or benzene/DMSO (7:3, 2.0 mL) for 24 h at 30°C under argon atmosphere. [b] **Conditions B**: 2-bromoalkanoate (0.2 mmol), alkyne (0.3 mmol), $NiBr_2$·diglyme (10 mol%), **L13** (15 mol%), DEMS (3.0 equiv), KF (3.0 equiv), and H_2O (2.5 equiv) in glyme/NMP (9:1, 4.0 mL) or THF/$PhCF_3$ (17:3, 4.0 mL) for 48 h at –20°C under argon atmosphere; reported yields are those of isolated products; regioisomeric ratios (r.r.) of those with diminished regioselectivity (r.r. <10:1) were determined by ^1H NMR of the crude reaction mixtures.

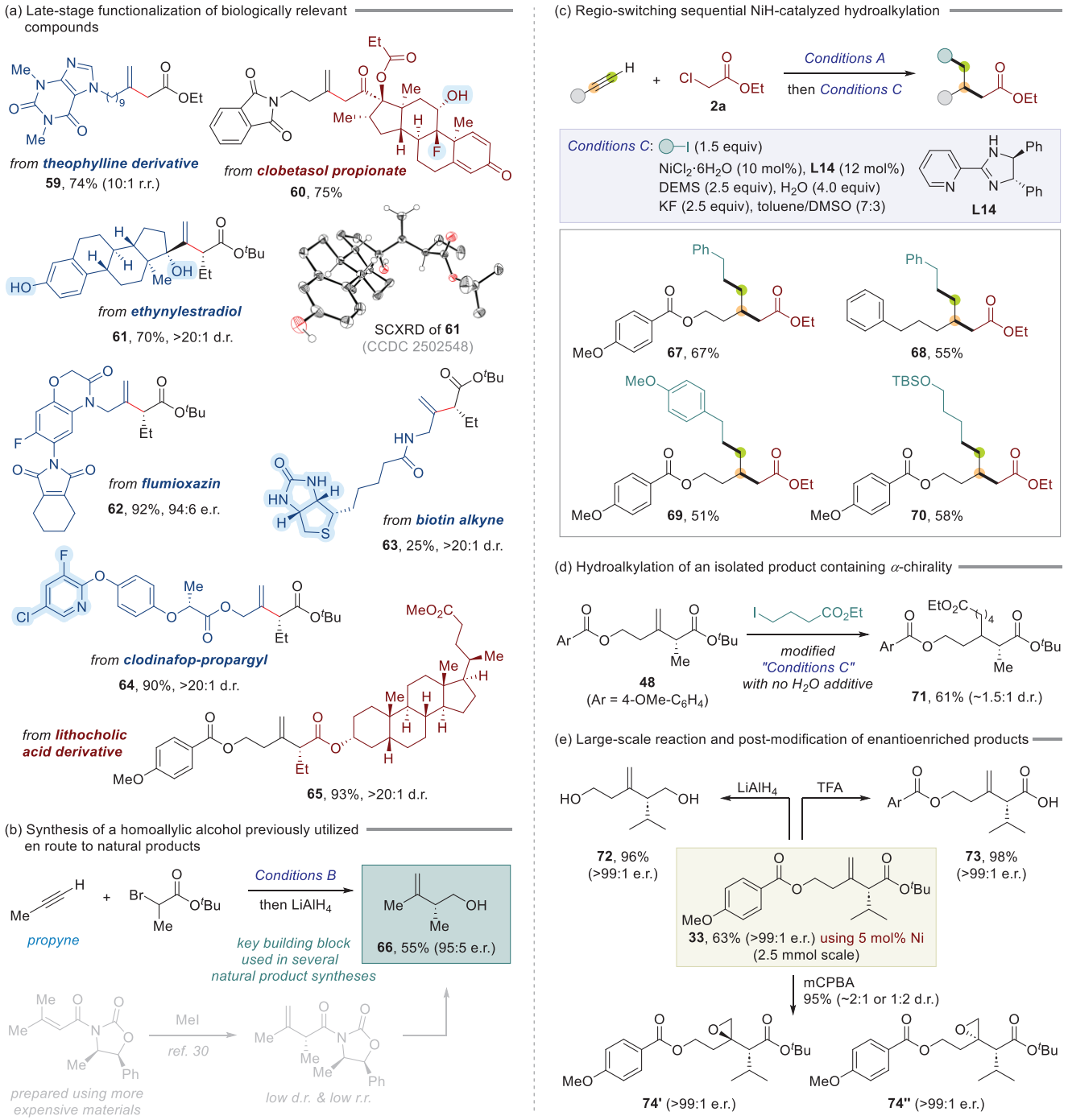

SCHEME 4 | Synthetic utility of the NiH-catalyzed α-alkenylation protocol. See Supporting Information for experimental details.

Extension of this asymmetric protocol to amide and ketone derivatives met with limited success, as the current system was precisely tailored to the steric profile of ester substrates. The poor performance of these analogs is likely attributable to ineffective catalyst–substrate coordination for amides and the stereochemical instability of ketone products (see Scheme S1).

2.3 | Applications

With both achiral and chiral systems proven highly effective, we next explored the feasibility of these transformations for late-stage functionalization (Scheme 4a). Interestingly, the reaction was applicable to biologically relevant molecules containing diverse functional motifs (**59–65**). For example, theophylline-derived alkyne and clobetasol propionate reacted efficiently with ethyl chloroacetate **2a** and phthalimide-based alkyne, respectively, furnishing the corresponding β-methylene carbonyl compounds **59** and **60** in good yields under achiral conditions. Asymmetric catalysis was also feasible for relatively complex alkynes such as ethynylestradiol (**61**), flumioxazin (**62**), biotin alkyne (**63**), and clodinafop-propargyl (**64**), of which the reactions with α-bromoester **4d** allowed for the Markovnikov addition with high stereoselectivities (>20:1 d.r. for **61, 63, 64** and 94:6 e.r. for

62). X-Ray crystallographic analysis of **61** revealed the stereochemical outcome of our asymmetric process, with the structure of the major diastereomer confirming the configuration at the bond-forming α-carbon relative to the pre-existing stereocenters. Complex α-bromoesters derived from lithocholic acid was also a viable substrate to enable the α-alkenylation reaction in excellent stereoselectivity (**65**; >20:1 d.r.). Notably, high yields were obtained except the reaction of biotin alkyne, further demonstrating the tolerance of various functional groups such as heterocyclic motifs, free hydroxyl, and fluoro groups.

The present transformation could also be applied to access chiral homoallylic alcohols through sequential reduction, as exemplified by the synthesis of enantioenriched alcohol **66** (Scheme 4b, top), which has been previously utilized as a key building block in the synthesis of several natural products [30,90–92]. This reaction was achieved by employing a gaseous alkyne reactant (propyne) in the initial NiH-catalyzed α-alkenylation, further highlighting the exceptional efficiency of the current system. In contrast to previous approaches that rely either on multi-step sequences from α-enantioenriched substrates [90–92] or on the pre-installation of chiral auxiliaries (Scheme 4b, bottom) [30], the present method provides **66** catalytically using commercially available starting materials in a concise two-step and single-purification procedure.

The resulting β-methylene unit also offers valuable opportunities for β-branching transformations. Although a wide range of alkene functionalization reactions are available [16–22], we sought to develop a sequential NiH protocol to access β-substituted carbonyl compounds via regio-switching sequential insertion (Scheme 4c). Further optimization was required for the anti-Markovnikov-selective hydroalkylation of β-methylene carbonyl compounds with alkyl iodides (see Tables S17 and S18), wherein pyridine-imidazoline ligand **L14** was found optimal. When combined with the achiral α-alkenylation conditions, this strategy furnished β-substituted carbonyl compounds (**67–70**) in moderate to good yields, again through a two-step and single-purification process using selected range of alkynes and alkyl iodides.

α-Substituted substrates were less compatible in the sequential approach; however, hydroalkylation of the isolated β-methylene product **48** successfully furnished the β-branched ester **71** in 61% yield (Scheme 4d). Asymmetric induction remained somehow challenging for the hydroalkylation of β-methylene units in both the sequential (Scheme 4c) and isolated approaches (Scheme 4d), the former affording nearly racemic mixtures and the latter exhibiting low diastereoselectivity (~1.5:1 d.r.). Nevertheless, this double hydroalkylation protocol provides an alternative dimension for accessing β-substituted carbonyl compounds. In particular, for those substrates bearing α-chirality, each of the resulting diastereomers may hold individual significance, illustrating the potential applicability of this approach in medicinal chemistry research.

The practicality of the present method was next demonstrated by a 2.5 mmol-scale reaction between alkyne **1** and the isopropyl carbonyl substrate, which furnished the corresponding β-methylene product **33** using only 5 mol% of the nickel precatalyst and 7.5 mol% of **L13** (Scheme 4e), with efficiency and selectivity comparable to those observed in small-scale reactions. Furthermore, the ester moiety in **33** could be readily transformed via reduction and deprotection to afford chiral diol **72** and carboxylic acid **73**, respectively, without any loss of enantiopurity (>99:1 e.r.). Epoxidation of **33** also proceeded smoothly to give the corresponding epoxide **74** in high yield, although the diastereoselectivity was not dictated by the pre-existing chirality (~2:1 d.r.). Nevertheless, the two diastereomers were separable, and their enantiopurity was confirmed to be retained.

2.4 | Mechanistic Investigation

With the proven synthetic utility in hand, we next carried out mechanistic investigations to elucidate the origins of the observed regio- and enantioselectivity (Scheme 5). To simplify the discussion, the achiral system was first examined to probe the plausible catalytic pathway and rationalize the regioselectivity outcome. Control experiments under modified achiral conditions using a combination of K_2HPO_4 (2.0 equiv) and D_2O (6.0 equiv) furnished the β-methylene product **3** without any deuterium incorporation, indicating that the reaction proceeds through the insertion of hydride rather than proton source (Scheme 5a).

One of the potential mechanisms for NiH-catalyzed hydroalkylation involves alkyne insertion into an alkyl-Ni species [93, 94]; however, this pathway appears less plausible in our system, given the relatively lower nucleophilicity of the α-carbon in esters. Indeed, DFT calculations revealed that such a carbonickellation process is energetically demanding with high energy barriers (see Scheme S2). We therefore investigated an alternative, more widely accepted hydronickellation pathway using 1-octyne as a model substrate, wherein the anti-Markovnikov and Markovnikov modes of insertion were compared (Scheme 5b). Notably, the Ni(I)H-based pathway was calculated to favor anti-Markovnikov hydronickellation (**Ni(I)_TS1_AM** *vs* **Ni(I)_TS1_M**; $\Delta\Delta G^{\ddagger}$ = 3.1 kcal mol^{-1}), whereas the Ni(II)H-based process preferred the Markovnikov pathway (**Ni(II)_TS1_M** *vs* **Ni(II)_TS1_AM**; $\Delta\Delta G^{\ddagger}$ = 1.9 kcal mol^{-1}).

This contrasting outcome can be attributed to an electronic change on the hydride ligand, as transition metal hydrides are known to exhibit amphoteric characters, with their hydridic or protic nature modulated by multiple factors [95–98]. In particular, the protic character of metal hydrides generally increases as the oxidation state of the central metal rises. Our natural bond orbital (NBO) analysis indeed supports this trend: the computed natural charges show that the hydrogen atom bears a partial negative charge in the Ni(I)H system when bound to the alkyne (**Ni(I)_int1_M** and **Ni(I)_int1_AM**), whereas it carries a partial positive charge in the Ni(II)H system (**Ni(II)_int1_M** and **Ni(II)_int1_AM**). Consequently, the electron-richer terminal carbon of the alkyne would electronically favor the interaction with the partially acidic hydrogen in the Ni(II)H species, thus leading to the observed Markovnikov-selectivity via highly endergonic hydronickellation process. Conversely, in this Ni(II)H manifold, diverting the reaction toward anti-Markovnikov selectivity appears challenging. While steric factors may influence regioselectivity to some extent, effective control for the access to the linear products would likely require a catalytic system operating via Ni(I)H. The predominance of Ni(II)H catalysis over Ni(I)H in our system may arise from the oxidizing nature of

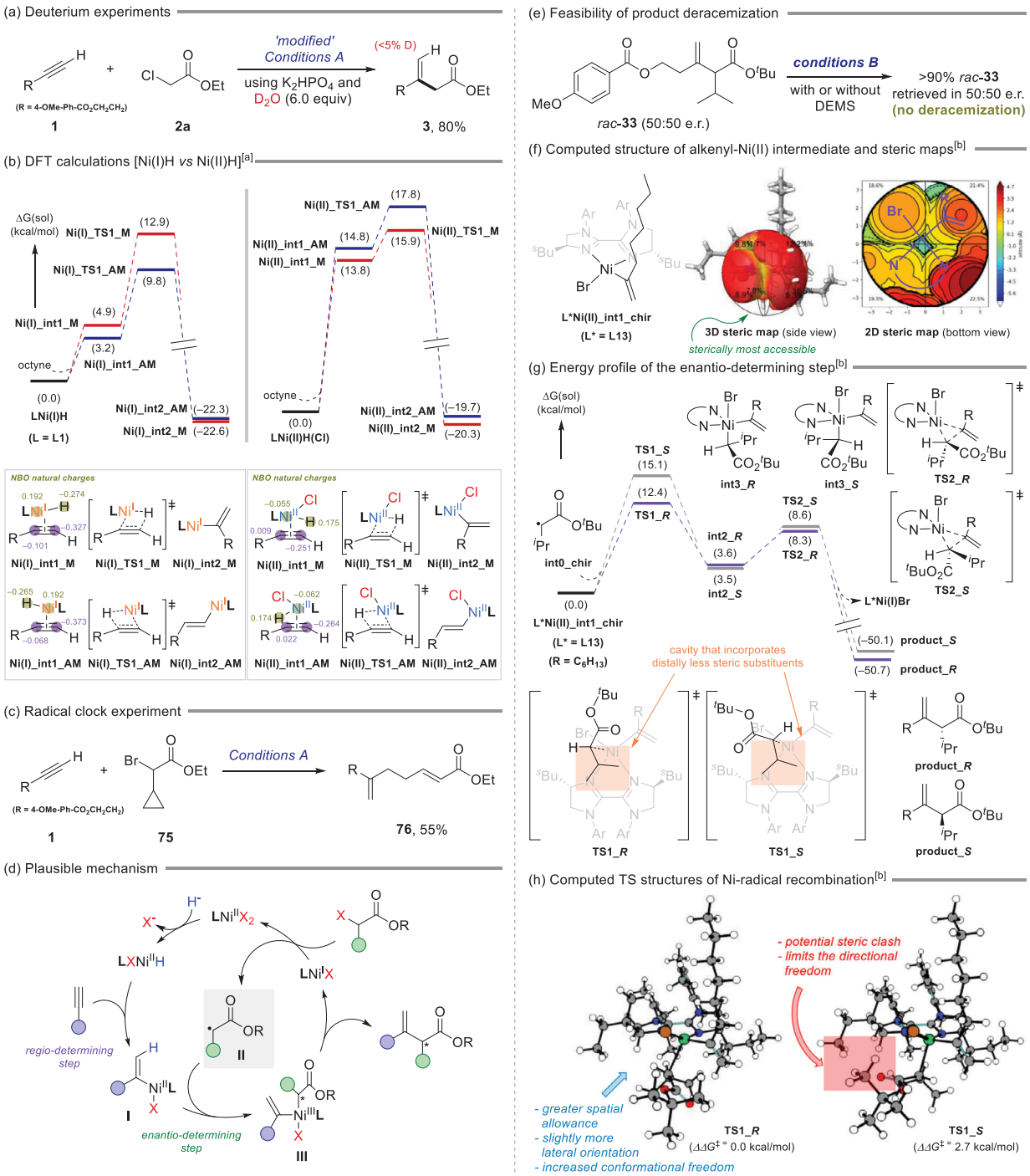

SCHEME 5 | Mechanistic investigations. [a] Energies calculated at the M06/6-311+G**|SDD(Ni)/SMD(toluene)// M06/6-31G**| SDD(Ni) level of theory. [b] Energies calculated at the M06/6-311+G**|SDD(Ni)/SMD(THF)// M06/6-31G**|SDD(Ni) level of theory.

the α-halocarbonyl substrates, which presumably oxidize Ni(I) intermediates to Ni(II) rapidly while being reduced themselves to the corresponding alkyl radicals.

The feasibility of such a single-electron transfer was examined through radical clock experiments employing the cyclopropyl-substituted α-halocarbonyl substrate **75** in reaction with alkyne **1** (Scheme 5c). Under the optimized achiral conditions, ring-opened product **76** was obtained in 55% yield, supporting the intermediacy of an α-carbon radical. Combining these experimental and computational results, a plausible Ni(II)H-based mechanism is depicted in Scheme 5d. As discussed above, alkyne undergoes Markovnikov-selective migratory insertion into the in situ-generated Ni(II)H to furnish the alkenyl-Ni intermediate **I**. This species then captures the α-carbon radical **II**, generated via single-electron reduction of the α-halocarbonyl substrate by a transient Ni(I) species. Subsequent reductive elimination from the resulting Ni(III) intermediate **III** delivers the β-methylene

product. Crucially, Ni(I)X is regenerated within the catalytic cycle to sustain the single-electron transfer with α-halocarbonyl substrate, although its initial formation likely stems from the partial reduction of Ni(II) to Ni(0) by silanes, followed by comproportionation with the remaining Ni(II) [99]. In an effort to experimentally substantiate this overall mechanistic picture, the synthesis of the key alkenyl-Ni intermediate proved challenging due to its inherent instability (see Figure S1); nonetheless, DFT calculations indicate that the proposed Ni(II)H-based mechanism is energetically feasible (see Scheme S3 for the full energy profile).

Finally, we sought to identify the catalyst features governing enantioselectivity, a mechanistic aspect that has rarely been exploited in related NiH-catalyzed enantioconvergent C–C bond-forming reactions. Although our system operates via a distinct catalytic manifold compared to recent photoredox-mediated α-deracemization strategies [100–104], the possibility of post-synthetic stereoconvergence could not be completely excluded. To probe this, a racemic mixture of product **33** (*rac*-**33**) was subjected to the standard asymmetric conditions, both in the presence and absence of a silane source (Scheme 5e). These control experiments revealed that the enantiomeric ratio remained unchanged (50:50), confirming the configurational stability of the α-stereocenter under the reaction conditions. This result indicates that the observed enantioselectivity originates from a stereoselective Ni-radical recombination step, rather than via thermodynamic equilibration of nonselectively formed products.

Accordingly, DFT calculations were further carried out to elucidate how the catalyst establishes the chiral environment, using **L13** as the model ligand. The structure of the alkenyl-Ni intermediate (**L*Ni(II)_int1_chir**) was first optimized, and its 3D steric map revealed an accessible region for the radical to approach at the lower left part when oriented as shown in Scheme 5f. The corresponding 2D steric map (bottom view) also indicated a small cavity extending inward toward the ligand backbone near the coordinating nitrogen on the left-hand side, which is likely capable of accommodating substituents that are less sterically demanding at their distal positions.

Indeed, the Ni-radical recombination with the isopropyl-based α-carbon radical (**int0_chir**) was calculated to occur at this specific site (Scheme 5g). While the ester functionality itself is essential for stereocontrol, the bulky *tert*-butyl *O*-substituent serves as a critical handle for restricting the approach trajectory. Specifically, directing this distal steric group toward the cavity causes significant steric repulsion at the ligand backbone, whereas α-alkyl substituents, being proximal to the radical center, can be accommodated within the cavity with less steric interference. Consistent with this hypothesis, two transition states were located to give relatively lower energies, in which the distal *tert*-butyl group is oriented away from the cavity (**TS1_*R*** and **TS1_*S***; see Scheme S4 for additional computed transition states). Among these, the transition state leading to the major (*R*)-configured isomer was energetically favored (**TS1_*R***, $\Delta\Delta G^{\ddagger}$ = 2.7 kcal mol^{-1}). The subsequent reductive elimination steps for both pathways were found to have relatively lower activation barriers (**TS2_*R*** and **TS2_*S***; see Scheme S5 for additional computed transition states), further supporting that the preceding Ni-radical recombination step serves as the enantio-determining step.

Given the absence of any stabilizing secondary interactions, the kinetic preference for the major pathway can be rationalized primarily by steric factors. Further examination of the computed structures for **TS1_*R*** and **TS1_*S*** revealed that the *sec*-butyl group on the left side of the ligand might also contribute to steric congestion to some extent (Scheme 5h). When the isopropyl substituent occupies the cavity, the *tert*-butyl ester in **TS1_*S*** is oriented slightly toward the left portion of the ligand, whose steric clash restricts the directional freedom as the radical approaches the metal center. In contrast, **TS1_*R*** features a small hydrogen substituent placed toward the oxazoline part of the ligand, which provides greater spatial allowance for the alkyl radical to approach with increased directional freedom. As a result, conformational flexibility within the cavity is enhanced, leading to reduced steric repulsion and correspondingly greater stabilization (see Tables S19 and S20 for summarized energy components of all DFT-optimized structures). This mechanistic picture not only rationalizes the observed enantioselectivity but may also guide the systematic development of further asymmetric transformations based on Ni-radical recombination.

3 | Conclusion

In conclusion, we have developed a NiH-catalyzed enantioconvergent α-alkenylation of carbonyl compounds with alkynes, providing a direct and general approach to α-chiral β-methylene carbonyl frameworks. The reaction proceeds via Markovnikov-selective alkyne hydronickellation followed by Ni-radical recombination, enabling highly regio- and enantioselective C–C bond formation across a broad substrate scope. The protocol exhibits excellent functional group tolerance, accommodates both achiral and chiral systems, and is amenable to late-stage functionalization of complex, biologically relevant molecules. The regio-switching sequential hydroalkylation protocol further underscores the versatility of the present system, enabling the construction of β-substituted products with increased molecular complexity. Mechanistic experiments and DFT calculations collectively support a Ni(II)H-centered catalytic cycle, in which the partially protic character of Ni(II)H dictates regioselectivity, while the Ni-radical recombination step governs enantiodiscrimination. The present study expands the conceptual boundaries of hydronickellation chemistry and paves the way for future development of stereoselective hydrofunctionalization reactions.

Acknowledgments

This work was supported by the National Research Foundation of Korea (NRF) grant funded by the Korea government (MSIT) (RS-2024-00454580 and RS-2025-00518096), and also by the DGIST Start-up Fund Program of the Ministry of Science and ICT (2023040012). The authors thank Prof. Sunggi Lee (DGIST), Prof. Byunghyuck Jung (DGIST), and their research groups for kindly sharing chemicals and granting access to their experimental facilities. Computational work for this research was performed on the supercomputing resources in the Supercomputing AI Education and Research Center (DGIST), partly supported by Grand Challenging Project. The authors also acknowledge Miss Jeonga Jeon (DGIST) for assistance with x-ray crystallographic analysis [105], Dr. Xiang Lyu (IBS) for assistance with polarimetric measurements, and Prof. Yoonsu Park (KAIST) and Mr. Dong Hyeon Kim (KAIST) for high resolution mass spectrometry (HRMS) analysis of selected compounds.

Conflicts of Interest

The authors declare no conflicts of interest.

Data Availability Statement

The data that support the findings of this study are available from the corresponding author upon reasonable request.

References

1. T. Qiao, Y. Wang, S. Zheng, H. Kang, and G. Liang, "Total Syntheses of Norrisolide-Type Spongian Diterpenes Cheloviolene C, Seconorrisolide B, and Seconorrisolide C," *Angewandte Chemie International Edition* 59 (2020): 14111–14114, https://doi.org/10.1002/anie.202005600.

2. H.-X. Huang, F. Mi, C. Li, et al., "Total Synthesis of Liangshanone," *Angewandte Chemie International Edition* 59 (2020): 23609–23614, https://doi.org/10.1002/anie.202011923.

3. J. Guo, B. Li, W. Ma, M. Pitchakuntla, and Y. Jia, "Total Synthesis of (−)-Glaucocalyxin A," *Angewandte Chemie International Edition* 59 (2020): 15195–15198, https://doi.org/10.1002/anie.202005932.

4. Y. Zhang, Y. Ji, I. Franzoni, et al., "Enantioselective Total Synthesis of Berkeleyone A and Preaustinoids," *Angewandte Chemie International Edition* 60 (2021): 14869–14874, https://doi.org/10.1002/anie.202104014.

5. S. Jin, X. Zhao, and D. Ma, "Divergent Total Syntheses of Napelline-Type C20-Diterpenoid Alkaloids: (−)-Napelline, (+)-Dehydronapelline, (−)-Songorine, (−)-Songoramine, (−)-Acoapetaldine D, and (−)-Liangshanone," *Journal of the American Chemical Society* 144 (2022): 15355–15362, https://doi.org/10.1021/jacs.2c06738.

6. H. Cheng, Z. Zhang, H. Yao, W. Zhang, J. Yu, and R. Tong, "Unified Asymmetric Total Syntheses of (−)-Alotaketals A–D and (−)-Phorbaketal A," *Angewandte Chemie International Edition* 56 (2017): 9096–9100, https://doi.org/10.1002/anie.201704628.

7. Y. Chen, W. Zhang, L. Ren, J. Li, and A. Li, "Total Syntheses of Daphenylline, Daphnipaxianine A, and Himalenine D," *Angewandte Chemie International Edition* 57 (2018): 952–956, https://doi.org/10.1002/anie.201711482.

8. N. A. Godfrey, D. J. Schatz, and S. V. Pronin, "Twelve-Step Asymmetric Synthesis of (−)-Nodulisporic Acid C," *Journal of the American Chemical Society* 140 (2018): 12770–12774, https://doi.org/10.1021/jacs.8b09965.

9. C. Peng, P. Arya, Z. Zhou, and S. A. Snyder, "A Concise Total Synthesis of (+)-Waihoensene Guided by Quaternary Center Analysis," *Angewandte Chemie International Edition* 59 (2020): 13521–13525, https://doi.org/10.1002/anie.202004177.

10. M. Haider, G. Sennari, A. Eggert, and R. Sarpong, "Total Synthesis of the Cephalotaxus Norditerpenoids (±)-Cephanolides A–D," *Journal of the American Chemical Society* 143 (2021): 2710–2715, https://doi.org/10.1021/jacs.1c00293.

11. Z. Ren, Z. Sun, Y. Li, et al., "Total Synthesis of (+)-3-Deoxyfortalpinoid F, (+)-Fortalpinoid A, and (+)-Cephinoid H," *Angewandte Chemie International Edition* 60 (2021): 18572–18576, https://doi.org/10.1002/anie.202108034.

12. Y. Zhao, J. Hu, R. Chen, F. Xiong, H. Xie, and H. Ding, "Divergent Total Syntheses of (−)-Crinipellins Facilitated by a HAT-Initiated Dowd–Beckwith Rearrangement," *Journal of the American Chemical Society* 144 (2022): 2495–2500, https://doi.org/10.1021/jacs.1c13370.

13. T. Ma, H. Cheng, M. Pitchakuntla, W. Ma, and Y. Jia, "Total Synthesis of (−)-Principinol C," *Journal of the American Chemical Society* 144 (2022): 20196–20200, https://doi.org/10.1021/jacs.2c08694.

14. R. J. Zachmann, K. Yahata, M. Holzheimer, M. Jarret, C. Wirtz, and A. Fürstner, "Total Syntheses of Nominal and Actual Prorocentin," *Journal of the American Chemical Society* 145 (2023): 2584–2595, https://doi.org/10.1021/jacs.2c12529.

15. R. Kučera, S. R. Ellis, K. Yamazaki, et al., "Enantioselective Total Synthesis of (−)-Himalensine A via a Palladium and 4-Hydroxyproline Co-Catalyzed Desymmetrization of Vinyl-Bromide-Tethered Cyclohexanones," *Journal of the American Chemical Society* 145 (2023): 5422–5430, https://doi.org/10.1021/jacs.2c13710.

16. J. V. Obligacion and P. J. Chirik, "Earth-abundant Transition Metal Catalysts for Alkene Hydrosilylation and Hydroboration," *Nature Reviews Chemistry* 2 (2018): 15–34, https://doi.org/10.1038/s41570-018-0001-2.

17. J. Chen and Z. Lu, "Asymmetric Hydrofunctionalization of Minimally Functionalized Alkenes via Earth Abundant Transition Metal Catalysis," *Organic Chemistry Frontiers* 5 (2018): 260–272, https://doi.org/10.1039/C7QO00613F.

18. H. Jiang and A. Studer, "Intermolecular Radical Carboamination of Alkenes," *Chemical Society Review* 49 (2020): 1790–1811, https://doi.org/10.1039/C9CS00692C.

19. J. Escorihuela, A. Lledós, and G. Ujaque, "Anti-Markovnikov Intermolecular Hydroamination of Alkenes and Alkynes: A Mechanistic View," *Chemical Review* 123 (2023): 9139–9203, https://doi.org/10.1021/acs.chemrev.2c00482.

20. Z.-L. Zhou, Y. Zhang, P.-Z. Cui, and J.-H. Li, "Photo-/Electrocatalytic Difunctionalization of Alkenes Enabled by C−H Radical Functionalization," *Chemistry–A European Journal* 30 (2024): e202402458, https://doi.org/10.1002/chem.202402458.

21. A. R. Gogoi, Á. Rentería-Gómez, T.-D. Tan, J. W. Ng, M. J. Koh, and O. Gutierrez, "Iron-catalysed Radical Difunctionalization of alkenes," *Nature Synthesis* 4 (2025): 1036–1055, https://doi.org/10.1038/s44160-025-00860-1.

22. Y. Wang, Z.-P. Bao, X.-D. Mao, M. Hou, and X.-F. Wu, "Intermolecular 1,2-difunctionalization of Alkenes," *Chemical Society Reviews* 54 (2025): 9530–9573, https://doi.org/10.1039/D5CS00670H.

23. P. D. Walker, A. N. M. Weir, C. L. Willis, and M. P. Crump, "Polyketide β-branching: Diversity, Mechanism and Selectivity," *Natural Product Reports* 38 (2021): 723–756, https://doi.org/10.1039/D0NP00045K.

24. Y. Yamamoto, S. Hatsuya, and J.-I. Yamada, "Diastereo- and Regioselective Aldol Condensation by Trapping Dienolates with Tin," *Journal of the Chemical Society, Chemical Communications* (1987): 561–562, https://doi.org/10.1039/c39870000561.

25. M. A. Battiste, J. R. Rocca, R. L. Wydra, J. H. Tumlinson, and T. Chuman, "Total Synthesis and Structure Proof of (3E,8E)-suspensolide," *Tetrahedron Letters* 29 (1988): 6565–6568, https://doi.org/10.1016/S0040-4039(00)82398-9.

26. M. Yamaguchi, M. Hamada, S. Kawasaki, and T. Minami, "A Regio- and Stereoselective Michael Addition of Amide Dienolates to α,β-Unsaturated Esters," *Chemistry Letters* 15 (2006): 1085–1088, https://doi.org/10.1246/cl.1986.1085.

27. K. V. Chuang, C. Xu, and S. E. Reisman, "A 15-step Synthesis of (+)-ryanodol," *Science* 353 (2016): 912–915, https://doi.org/10.1126/science.aag1028.

28. X. Chen, Y. Lu, Z. Guan, et al., "Synthesis of Succinimides via Intramolecular Alder-Ene Reaction of 1,6-Enynes," *Organic Letters* 23 (2021): 3173–3178, https://doi.org/10.1021/acs.orglett.1c00888.

29. A. Mondal, B. Satpathi, and S. S. V. Ramasastry, "Phosphine-Catalyzed Intramolecular Vinylogous Aldol Reaction of α-Substituted Enones," *Organic Letters* 24 (2022): 256–261, https://doi.org/10.1021/acs.orglett.1c03913.

30. D. M. Walba, W. N. Thurmes, and R. C. Haltiwanger, "A Highly Stereocontrolled Route to the monensin spiroketal Ring System," *Journal of Organic Chemistry* 53 (1988): 1046–1056, https://doi.org/10.1021/jo00240a022.

31. G. Cardillo, A. D'Amico, M. Orena, and S. Sandri, "Diastereoselective Alkylation of 3-acylimidazolidin-2-ones: Synthesis of (R)- and (S)-lavandulol," *Journal of Organic Chemistry* 53 (1988): 2354–2356, https://doi.org/10.1021/jo00245a043.

32. L.-J. Gao, X.-Y. Zhao, M. Vandewalle, and P. D. Clercq, "Convergent Synthesis of 1α-Hydroxyvitamin D5," *European Journal of Organic Chemistry* 2000 (2000): 2755–2759, https://doi.org/10.1002/1099-0690(200008)2000:15⟨2755::AID-EJOC2755⟩3.0.CO;2-G.

33. G. E. Keck, C. E. Knutson, and S. A. Wiles, "Total Synthesis of the Immunosupressant (−)-Pironetin (PA48153C)," *Organic Letters* 3 (2001): 707–710, https://doi.org/10.1021/ol015531m.

34. M. S. Kwon, S. H. Sim, Y. K. Chung, and E. Lee, "Synthetic Studies on Soft Coral Norcembranolides: Total Synthesis of (+)-10-epigyrosanolide E," *Tetrahedron* 67 (2011): 10179–10185, https://doi.org/10.1016/j.tet.2011.09.011.

35. J. H. Boyce, V. Eschenbrenner-Lux, and J. A. Porco Jr., "Syntheses of (+)-30- epi -, (−)-6- epi -, (±)-6,30- epi -13,14-Didehydroxyisogarcinol and (±)-6,30- epi -Garcimultiflorone A Utilizing Highly Diastereoselective, Lewis Acid-Controlled Cyclizations," *Journal of the American Chemical Society* 138 (2016): 14789–14797, https://doi.org/10.1021/jacs.6b09727.

36. H. Takamura, Y. Sugitani, R. Morishita, and I. Kadota, "Total Synthesis of Scabrolide F," *Organic Letters* 24 (2022): 7845–7849, https://doi.org/10.1021/acs.orglett.2c03263.

37. E. M. Brun, S. Gil, and M. Parra, "Enantioselective α-alkylation of Unsaturated Carboxylic Acids Using a Chiral Lithium Amide," *Tetrahedron Asymmetry* 12 (2001): 915–921, https://doi.org/10.1016/S0957-4166(01)00152-5.

38. W. Zhang, Z. Zhang, J.-C. Tang, et al., "Total Synthesis of (+)-Haperforin G," *Journal of the American Chemical Society* 142 (2020): 19487–19492, https://doi.org/10.1021/jacs.0c10122.

39. Y. Ji, B. Hong, I. Franzoni, et al., "Enantioselective Total Synthesis of Hyperforin and Pyrohyperforin," *Angewandte Chemie International Edition* 61 (2022): e202116136, https://doi.org/10.1002/anie.202116136.

40. H. Tsuji, K.-I. Yamagata, Y. Itoh, K. Endo, M. Nakamura, and E. Nakamura, "Indium-Catalyzed Cycloisomerization of ω-Alkynyl-β-Ketoesters into Six- to Fifteen-Membered Rings," *Angewandte Chemie International Edition* 46 (2007): 8060–8062, https://doi.org/10.1002/anie.200702928.

41. Y. Itoh, H. Tsuji, K.-I. Yamagata, et al., "Efficient Formation of Ring Structures Utilizing Multisite Activation by Indium Catalysis," *Journal of the American Chemical Society* 130 (2008): 17161–17167, https://doi.org/10.1021/ja805657h.

42. M. Li, T. Yang, and D. J. Dixon, "Boronic Acid Catalyzed Ene Carbocyclization of Acetylenic Dicarbonyl Compounds," *Chemical Communications* 46 (2010): 2191–2193, https://doi.org/10.1039/b924899d.

43. H. Ito, H. Ohmiya, and M. Sawamura, "Construction of Methylenecycloheptane Frameworks through 7 -Exo-Dig Cyclization of Acetylenic Silyl Enol Ethers Catalyzed by Triethynylphosphine–Gold Complex," *Organic Letters* 12 (2010): 4380–4383, https://doi.org/10.1021/ol101860j.

44. T. Iwai, H. Okochi, H. Ito, and M. Sawamura, "Construction of Eight-Membered Carbocycles through Gold Catalysis with Acetylene-Tethered Silyl Enol Ethers," *Angewandte Chemie International Edition* 52 (2013): 4239–4242, https://doi.org/10.1002/anie.201300265.

45. C. F. Heinrich, I. Fabre, and L. Miesch, "Silver-Catalyzed 7 -Exo-Dig Cyclization of Silylenolether-Ynesulfonamides," *Angewandte Chemie International Edition* 55 (2016): 5170–5174, https://doi.org/10.1002/anie.201510708.

46. A. J. Frontier, S. Raghavan, and S. J. Danishefsky, "Stereocontrolled Total Synthesis of Hispidospermidin," *Journal of the American Chemical Society* 119 (1997): 6686–6687, https://doi.org/10.1021/ja970889s.

47. K. C. Nicolaou, G. S. Tria, and D. J. Edmonds, "Total Synthesis of Platencin," *Angewandte Chemie International Edition* 47 (2008): 1780–1783, https://doi.org/10.1002/anie.200800066.

48. Y. Han, L. Zhu, Y. Gao, and C.-S. Lee, "A Highly Convergent Cascade Cyclization to Cis-Hydrindanes with all-Carbon Quaternary Centers and Its Application in the Synthesis of the Aglycon of Dendronobiloside A," *Organic Letters* 13 (2011): 588–591, https://doi.org/10.1021/ol102781p.

49. Z. Lu, Y. Li, J. Deng, and A. Li, "Total Synthesis of the Daphniphyllum Alkaloid Daphenylline," *Nature Chemistry* 5 (2013): 679–684, https://doi.org/10.1038/nchem.1694.

50. F. W. W. Hartrampf, T. Furukawa, and D. Trauner, "A Conia-Ene-Type Cyclization under Basic Conditions Enables an Efficient Synthesis of (−)-Lycoposerramine R," *Angewandte Chemie International Edition* 56 (2017): 893–896, https://doi.org/10.1002/anie.201610021.

51. L. Allievi, S. Dhambri, R. Sun, et al., "Gold(I)-Catalyzed 7-exo-dig Cyclization: A Key Step to Access the Bicyclo[4.2.1]Nonane Skeleton of Vibsatin A, a Neurotrophic Diterpenoid," *Organic Letters* 23 (2021): 5218–5222, https://doi.org/10.1021/acs.orglett.1c01757.

52. B. M. Trost, G. Zhang, H. Gholami, and D. Zell, "Total Synthesis of Kadcoccinic Acid A Trimethyl Ester," *Journal of the American Chemical Society* 143 (2021): 12286–12293, https://doi.org/10.1021/jacs.1c05521.

53. B. K. Corkey and F. D. Toste, "Catalytic Enantioselective Conia-Ene Reaction," *Journal of the American Chemical Society* 127 (2005): 17168–17169, https://doi.org/10.1021/ja055059q.

54. T. Yang, A. Ferrali, F. Sladojevich, L. Campbell, and D. J. Dixon, "Brønsted Base/Lewis Acid Cooperative Catalysis in the Enantioselective Conia-Ene Reaction," *Journal of the American Chemical Society* 131 (2009): 9140–9141, https://doi.org/10.1021/ja9004859.

55. F. Sladojevich, Á. L. Fuentes de Arriba, I. Ortín, et al., "Mechanistic Investigations into the Enantioselective Conia-Ene Reaction Catalyzed by Cinchona-Derived Amino Urea Pre-Catalysts and Cu I," *Chemistry–A European Journal* 19 (2013): 14286–14295, https://doi.org/10.1002/chem.201200832.

56. S. Shaw and J. D. White, "A New Iron(III)–Salen Catalyst for Enantioselective Conia-ene Carbocyclization," *Journal of the American Chemical Society* 136 (2014): 13578–13581, https://doi.org/10.1021/ja507853f.

57. R. Manzano, S. Datta, R. S. Paton, and D. J. Dixon, "Enantioselective Silver and Amine Co-Catalyzed Desymmetrizing Cycloisomerization of Alkyne-Linked Cyclohexanones," *Angewandte Chemie International Edition* 56 (2017): 5834–5838, https://doi.org/10.1002/anie.201612048.

58. Y. Xu, Q. Sun, T.-D. Tan, et al., "Organocatalytic Enantioselective Conia-Ene-Type Carbocyclization of Ynamide Cyclohexanones: Regiodivergent Synthesis of Morphans and Normorphans," *Angewandte Chemie International Edition* 58 (2019): 16252–16259, https://doi.org/10.1002/anie.201908495.

59. K. Kaneda, K. Motokura, N. Nakagiri, T. Mizugaki, and K. Jitsukawa, "Recyclable Indium Catalysts for Additions of 1,3-dicarbonyl Compounds to Unactivated Alkynes Affected by Structure and Acid Strength of Solid Supports," *Green Chemistry* 10 (2008): 1231–1234, https://doi.org/10.1039/b810490e.

60. G. K. Verma, M. Rawat, and D. S. Rawat, "Cobalt-Catalysed C–C Bond Formation and [2+2+2] Annulation of 1,3-Dicarbonyls to Terminal Alkynes," *European Journal of Organic Chemistry* 2019 (2019): 4101–4104, https://doi.org/10.1002/ejoc.201900725.

61. A. J. Jordan, G. Lalic, and J. P. Sadighi, "Coinage Metal Hydrides: Synthesis, Characterization, and Reactivity," *Chemical Reviews* 116 (2016): 8318–8372, https://doi.org/10.1021/acs.chemrev.6b00366.

62. N. A. Eberhardt and H. Guan, "Nickel Hydride Complexes," *Chemical Reviews* 116 (2016): 8373–8426, https://doi.org/10.1021/acs.chemrev.6b00259.

63. Y. Hu, A. P. Shaw, D. P. Estes, and J. R. Norton, "Transition-Metal Hydride Radical Cations," *Chemical Reviews* 116 (2016): 8427–8462, https://doi.org/10.1021/acs.chemrev.5b00532.

64. S. W. M. Crossley, C. Obradors, R. M. Martinez, and R. A. Shenvi, "Mn-, Fe-, and Co-Catalyzed Radical Hydrofunctionalizations of Olefins," *Chemical Reviews* 116 (2016): 8912–9000, https://doi.org/10.1021/acs.chemrev.6b00334.

65. Y. Wang, Y. He, and S. Zhu, "Nickel-Catalyzed Migratory Cross-Coupling Reactions: New Opportunities for Selective C–H Functionalization," *Accounts of Chemical Research* 56 (2023): 3475–3491, https://doi.org/10.1021/acs.accounts.3c00540.

66. B. C. Lee, C.-F. Liu, L. Q. H. Lin, et al., "N-Heterocyclic Carbenes as Privileged Ligands for Nickel-catalysed Alkene Functionalisation," *Chemical Society Reviews* 52 (2023): 2946–2991, https://doi.org/10.1039/D2CS00972B.

67. Y. Li, X. Lu, and Y. Fu, "Recent Advances in Cobalt-Catalyzed Regio- or Stereoselective Hydrofunctionalization of Alkenes and Alkynes," *CCS Chemistry* 6 (2024): 1130–1156, https://doi.org/10.31635/ccschem.024.202303678.

68. J. Chen, W.-T. Wei, Z. Li, and Z. Lu, "Metal-catalyzed Markovnikov-type Selective Hydrofunctionalization of Terminal Alkynes," *Chemical Society Reviews* 53 (2024): 7566–7589, https://doi.org/10.1039/D4CS00167B.

69. B. Liu and Q. Liu, "Cobalt-Catalyzed Hydroalkylation of Alkenes and Alkynes: Advantages and Opportunities," *Chemcatchem* 16 (2024): e202301188, https://doi.org/10.1002/cctc.202301188.

70. C. Lee, D. Lee, S. Y. Hong, B. Jung, and S. Seo, "Recent Advances in Earth-abundant Transition Metal-catalyzed Dihydrosilylation of Terminal Alkynes," *Frontier Chemistry* 12 (2024): 1411140, https://doi.org/10.3389/fchem.2024.1411140.

71. A. Hazra, J. A. Kephart, A. Velian, and G. Lalic, "Hydroalkylation of Alkynes: Functionalization of the Alkenyl Copper Intermediate through Single Electron Transfer Chemistry," *Journal of the American Chemical Society* 143 (2021): 7903–7908, https://doi.org/10.1021/jacs.1c03396.

72. Y. Li, D. Liu, L. Wan, J.-Y. Zhang, X. Lu, and Y. Fu, "Ligand-Controlled Cobalt-Catalyzed Regiodivergent Alkyne Hydroalkylation," *Journal of the American Chemical Society* 144 (2022): 13961–13972, https://doi.org/10.1021/jacs.2c06279.

73. X.-Y. Sun, B.-Y. Yao, B. Xuan, L.-J. Xiao, and Q.-L. Zhou, "Recent advances in nickel-catalyzed asymmetric hydrofunctionalization of alkenes," *Chem Catalysis* 2 (2022): 3140–3162, https://doi.org/10.1016/j.checat.2022.10.020.

74. F. Zhou, J. Zhu, Y. Zhang, and S. Zhu, "NiH-Catalyzed Reductive Relay Hydroalkylation: A Strategy for the Remote C(sp3)−H Alkylation of Alkenes," *Angewandte Chemie International Edition* 57 (2018): 4058–4062, https://doi.org/10.1002/anie.201712731.

75. J.-W. Wang, Y. Li, W. Nie, et al., "Catalytic Asymmetric Reductive Hydroalkylation of Enamides and Enecarbamates to Chiral Aliphatic Amines," *Nature Communications* 12 (2021): 1313, https://doi.org/10.1038/s41467-021-21600-x.

76. F. Zhou and S. Zhu, "Catalytic Asymmetric Hydroalkylation of α,β-Unsaturated Amides Enabled by Regio-Reversed and Enantiodifferentiating Syn -Hydronickellation," *ACS Catalysis* 11 (2021): 8766–8773, https://doi.org/10.1021/acscatal.1c02299.

77. J.-W. Wang, Z. Li, D. Liu, J.-Y. Zhang, X. Lu, and Y. Fu, "Nickel-Catalyzed Remote Asymmetric Hydroalkylation of Alkenyl Ethers to Access Ethers of Chiral Dialkyl Carbinols," *Journal of the American Chemical Society* 145 (2023): 10411–10421, https://doi.org/10.1021/jacs.3c02950.

78. C. Fan, U. Dhawa, D. Qian, D. Sakic, J. Morel, and X. Hu, "Regiodivergent and Enantioselective Synthesis of Cyclic Sulfones via Ligand-Controlled Nickel-Catalyzed Hydroalkylation," *Angewandte Chemie International Edition* 63 (2024): e202406767, https://doi.org/10.1002/anie.202406767.

79. J.-W. Wang, Q.-W. Zhu, D. Liu, et al., "Nickel-Catalyzed α-Selective Hydroalkylation of Vinylarenes," *Angewandte Chemie International Edition* 63 (2024): e202413074, https://doi.org/10.1002/anie.202413074.

80. G. Ju, X. Yan, H. Bai, et al., "Stereodivergent Construction of Non-adjacent Stereocentres via Migratory Functionalization of alkenes," *Nature Chemistry* 18 (2026): 345–355, https://doi.org/10.1038/s41557-025-01994-7.

81. Z. Wang, H. Yin, and G. C. Fu, "Catalytic Enantioconvergent Coupling of Secondary and Tertiary Electrophiles with Olefins," *Nature* 563 (2018): 379–383, https://doi.org/10.1038/s41586-018-0669-y.

82. S.-Z. Sun, Y.-M. Cai, D.-L. Zhang, et al., "Enantioselective Deaminative Alkylation of Amino Acid Derivatives with Unactivated Olefins," *Journal of the American Chemical Society* 144 (2022): 1130–1137, https://doi.org/10.1021/jacs.1c12350.

83. F. Zhou, Y. Zhang, X. Xu, and S. Zhu, "NiH-Catalyzed Remote Asymmetric Hydroalkylation of Alkenes with Racemic α-Bromo Amides," *Angewandte Chemie International Edition* 58 (2019): 1754–1758, https://doi.org/10.1002/anie.201813222.

84. J. Hu, S. Su, H. Zhang, H. An, Y. Chen, and H. Gong, "Ligand-Controlled Stereodivergent α-Vinylation and α-Arylation of Peptide Backbones," *Journal of the American Chemical Society* 147 (2025): 38475–38483, https://doi.org/10.1021/jacs.5c11836.

85. A. Hossain and G. C. Fu, "Nickel-Catalyzed Asymmetric α-Alkenylations of Acyclic Amides That Provide Tertiary Stereocenters," *Journal of the American Chemical Society* 147 (2025): 40910–40916, https://doi.org/10.1021/jacs.5c14143.

86. X. Lyu, J. Zhang, D. Kim, S. Seo, and S. Chang, "Merging NiH Catalysis and Inner-Sphere Metal-Nitrenoid Transfer for Hydroamidation of Alkynes," *Journal of the American Chemical Society* 143 (2021): 5867–5877, https://doi.org/10.1021/jacs.1c01138.

87. H. Choi, X. Lyu, D. Kim, S. Seo, and S. Chang, "Endo-Selective Intramolecular Alkyne Hydroamidation Enabled by NiH Catalysis Incorporating Alkenylnickel Isomerization," *Journal of the American Chemical Society* 144 (2022): 10064–10074, https://doi.org/10.1021/jacs.2c03777.

88. X. Lyu, C. Seo, H. Jung, et al., "Intramolecular Hydroamidation of Alkenes Enabling Asymmetric Synthesis of β-lactams via Transposed NiH Catalysis," *Nature catalysis* 6 (2023): 784–795, https://doi.org/10.1038/s41929-023-01014-2.

89. C. Lee, J. H. Jeon, S. Lee, et al., "Nickel-Catalyzed Mono- and Dihydrosilylation of Aliphatic Alkynes in Aqueous and Aerobic Conditions," *ACS catalysis* 14 (2024): 5077–5087, https://doi.org/10.1021/acscatal.4c00109.

90. J. D. White, G. N. Reddy, and G. O. Spessard, "Total Synthesis of (-)-botryococcene," *Journal of the American Chemical Society* 110 (1988): 1624–1626, https://doi.org/10.1021/ja00213a047.

91. J. D. White, G. N. Reddy, and G. O. Spessard, "Total Synthesis of (–)-C 34-botryococcene, the Principal Triterpenoid Hydrocarbon of the Freshwater Alga Botryococcus Braunii," *Journal of the Chemical Society, Perkin Transactions 1* (1993): 759–767, https://doi.org/10.1039/P19930000759.

92. D. R. Williams, S. V. Plummer, and S. Patnaik, "Studies for the Enantiocontrolled Preparation of Substituted Tetrahydropyrans: Applications for the Synthesis of Leucascandrolide A Macrolactone," *Tetrahedron* 67 (2011): 5083–5097, https://doi.org/10.1016/j.tet.2011.05.020.

93. N. A. Till, R. T. Smith, and D. W. C. MacMillan, "Decarboxylative Hydroalkylation of Alkynes," *Journal of the American Chemical Society* 140 (2018): 5701–5705, https://doi.org/10.1021/jacs.8b02834.

94. Q. Gao, W.-C. Xu, X. Nie, et al., "Regio- and Enantioselective Nickel-Alkyl Catalyzed Hydroalkylation of Alkynes," *Nature Communications* 15 (2024): 6556, https://doi.org/10.1038/s41467-024-50947-0.

95. H. W. Walker, C. T. Kresge, P. C. Ford, and R. G. Pearson, "Rates of Deprotonation and pKa Values of Transition Metal Carbonyl Hydrides," *Journal of the American Chemical Society* 101 (1979): 7428–7429, https://doi.org/10.1021/ja00518a061.

96. R. H. Morris, "Estimating the Acidity of Transition Metal Hydride and Dihydrogen Complexes by Adding Ligand Acidity Constants," *Journal of the American Chemical Society* 136 (2014): 1948–1959, https://doi.org/10.1021/ja410718r.

97. R. H. Morris, "Brønsted–Lowry Acid Strength of Metal Hydride and Dihydrogen Complexes," *Chemical Reviews* 116 (2016): 8588–8654, https://doi.org/10.1021/acs.chemrev.5b00695.

98. E. S. Wiedner, M. B. Chambers, C. L. Pitman, R. M. Bullock, A. J. M. Miller, and A. M. Appel, "Thermodynamic Hydricity of Transition Metal Hydrides," *Chemical Reviews* 116 (2016): 8655–8692, https://doi.org/10.1021/acs.chemrev.6b00168.

99. C. S. Day and R. Martin, "Comproportionation and Disproportionation in Nickel and Copper Complexes," *Chemical Society Reviews* 52 (2023): 6601–6616, https://doi.org/10.1039/D2CS00494A.

100. N. Y. Shin, J. M. Ryss, X. Zhang, S. J. Miller, and R. R. Knowles, "Light—Driven Deracemization Enabled by Excited—State Electron Transfer," *Science* 366 (2019): 364–369, https://doi.org/10.1126/science.aay2204.

101. C. Zhang, A. Z. Gao, X. Nie, et al., "Catalytic α-Deracemization of Ketones Enabled by Photoredox Deprotonation and Enantioselective Protonation," *Journal of the American Chemical Society* 143 (2021): 13393–13400, https://doi.org/10.1021/jacs.1c06637.

102. Z. Gu, L. Zhang, H. Li, et al., "Deracemization through Sequential Photoredox-Neutral and Chiral Brønsted Acid Catalysis," *Angewandte Chemie International Edition* 61 (2022): e202211241, https://doi.org/10.1002/anie.202211241.

103. T. Pan, X. Jiang, M. Huang, L. Zhang, and S. Luo, "Visible Light-Promoted Deracemization of α-Amino Aldehyde by Synergistic Chiral Primary Amine and Hypervalent Iodine Catalysis," *Journal of the American Chemical Society* 147 (2025): 6280–6287, https://doi.org/10.1021/jacs.4c18407.

104. J. Y. Wang, E. Villalona, and R. R. Knowles, "Photocatalyst-Dependent Enantioselectivity in the Light-Driven Deracemization of Cyclic α-Aryl Ketones," *Journal of the American Chemical Society* 147 (2025): 15307–15317, https://doi.org/10.1021/jacs.5c00847.

105. Deposition numbers CCDC, 2502548 (for **61**) and 2514232 (for **Ni_DP**) contain the supplementary crystallographic data for this paper (see Tables S21 and S22). These data are provided free of charge by the joint Cambridge Crystallographic Data Centre and Fachinformationszentrum Karlsruhe Access Structures service.

Supporting Information

Additional supporting information can be found online in the Supporting Information section.

Supporting File 1: anie71837-sup-0001-SuppMat.pdf.